

The 8th International Conference on Energy and Environment Research ICEER 2021, 13–17
September

Image recognition method for frost sensing applications

Martim Aguiar, Pedro Dinis Gaspar*, Pedro Dinho da Silva

C-MAST, Center for Mechanical and Aerospace Science and Technologies, Faculty of Engineering, University of Beira Interior, Calçada Fonte do Lameiro, 6201-001 Covilhã, Portugal

Received 31 December 2021; accepted 10 January 2022

Available online xxx

Abstract

Frost formation in the heat exchangers of refrigeration systems is a well-documented phenomenon. This frost accumulation creates a thermally insulating barrier that can restrict, or even block, the airflow between fins, resulting in decreased efficiency and degradation of the food products. Several methods of frost detection and defrosting have been developed, although there is not an efficient mainstream method to measure and control frost formation. In previous works, the results of a small low-cost resistive sensor for frost detection were shown to be promising. This paper extends that research using computer vision to compare the results of this sensor with the frost formed on the heat exchanger, allowing for a better study of the sensor. This method allowed to trace and plot a frost formation curve of the sensor detected values.

© 2022 The Author(s). Published by Elsevier Ltd. This is an open access article under the CC BY license

(<http://creativecommons.org/licenses/by/4.0/>).

Peer-review under responsibility of the scientific committee of the 8th International Conference on Energy and Environment Research, ICEER, 2021.

Keywords: Computer vision; Defrosting; Frost formation; Frost sensing; Refrigeration

1. Introduction

Frost formation in air conditioning and refrigeration systems is still a problem that causes a significant decrease in efficiency. When used in light commercial systems, heat exchangers (HXs) have a large area-to-volume ratio. If subfreezing temperatures are demanded, a frost layer usually forms on the fin surface, Melo et al. [1], as shown on Fig. 1

This frost layer creates a thermal barrier that decreases the heat transfer between air and the refrigerant. Furthermore, the frost buildup restricts, or even blocks, the airflow passage between fins, if no defrost method is applied. This results in higher energy demand, and in extreme cases, system damage, Hermes et al. [2], besides the thermal performance reduction.

To reduce the problem, defrost methods are used, although additional energy might also be consumed for their operation, Wang et al. [3].

* Corresponding author.

E-mail address: dinis@ubi.pt (P.D. Gaspar).

<https://doi.org/10.1016/j.egy.2022.01.049>

2352-4847/© 2022 The Author(s). Published by Elsevier Ltd. This is an open access article under the CC BY license (<http://creativecommons.org/licenses/by/4.0/>).

Peer-review under responsibility of the scientific committee of the 8th International Conference on Energy and Environment Research, ICEER, 2021.

Nomenclature

HX	Heat exchanger
RGB	Red Green Blue color model
B&W	Black and White
ADC	Analog to Digital Converter

Restraint frost approaches various methods for the retardation of the frost formation, while frost removal acts upon the formed frost to remove it, Aguiar et al. [4]. Complexity, cost, and unreliable sensing/prediction methods make most of the defrosting methods difficult to implement in industrial systems. Timed defrost operations, one of the most used methods to control defrosting operations, must be timed for the worst-case scenario, not taking in consideration the fluctuation of parameters that influence frost formation. These fluctuations cause different frost formation along the day and season, that would require different defrosting cycle periods, Ge et al. [5].

Demand defrost tries to solve this problem by predicting frost formation. Either by computing the parameters that influence frost formation, measuring symptoms of frost accumulation, or directly measuring frost formation, Jarrett [6]. Several sensing methods have been studied to directly measure frost formation, using capacitive, photoelectric, piezoelectric, optic fiber and resistive sensors, Aguiar et al. [4], but to study the sensor accuracy, a precise frost detection method should be employed to cross the data between the sensor measurements, and the real frost formation.

1.1. Related works

Zhu et al. [7] used a method that applied computer vision to detect dryness, dew, and frost during the night. This method uses glass plates with a treatment that causes them to have visually distinct characteristics when dry, wet or frost is deposited on the surface. This method uses the completed local binary pattern to distinguish between surface textures and achieved a 90% accuracy.

Li et al. [8] used a novel imaging recognition method to detect frost in HXs and control defrosting operations with very promising results. This method captures an image and converts it to a Black and White (B&W) grayscale image, in which, each pixel has a value between 0 and 255. A threshold is then set, and pixel values above this threshold are considered as frost by the system. It was found that illumination can impact the measurements if not taken into consideration, which was partially solved by using an area for illumination recognition.

The necessity to apply a camera facing the HX (even though cameras can be placed in an angle, with a wide-angle lens) and illumination requirements might make it difficult to implement in a compact refrigeration system for real commercial application, but its reliability and accuracy throughout HX zones make it perfect for laboratory application, and data crossing with other sensing methods. The present work aims to use a computer vision method to detect frost formation and compare it to a frost detection sensor.

2. Materials and methods

The detection of water accumulation and frost formation in a HX can be measured by a simple, small, and low-cost resistive sensor. This sensor was developed in previous works, Aguiar et al. [9] and consists of two 0.5 mm copper electrodes joined and insulated through a cotton string that acts both as an electrical insulator, and moisture absorbent.

According to the material deposited between the sensor electrodes (air, water or ice), the voltage drop across sensor terminals will fluctuate due to the different electrical resistivity values. With this fluctuation, a relation to air, water and ice can be created. If the sensor is placed between the HX fins, and the electrodes are close enough for a voltage drop to be measured when a voltage is applied to the terminals, a characteristic voltage drop will be measured as water forms, and this voltage drop will increase as water freezes, and increase further as water evaporates during defrosting. A device based on this characteristic was developed by Gaspar et al. [10] and Caetano et al. [11]. The sensor resistance, and consequently the voltage drop, vary according to Eq. (1).

$$R = \rho \cdot L / A \quad (1)$$

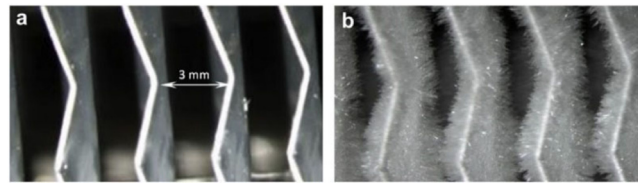


Fig. 1. HX fin before (a) and after (b) frost formation, Hermes et al. [2].

In which R [Ω] is the overall sensor resistance, ρ [$\Omega.m$] the resistivity that fluctuates with the material between the electrodes, L [m] the length of this material, or in this case, distance between electrodes, and A [m^2] the section area of the connection between electrodes. When water condenses on the HX surface, it is absorbed by the sensor’s cotton string, reducing the resistivity of the fabric, and decreasing the voltage drop on its terminals. As frost is formed, the resistivity increases, the voltage drop increases and frost is detected. When a defrosting operation is performed, water is again detected, until the HX is dry again. The sensor is clamped on one of the HX’s fins and is shown in Fig. 2.

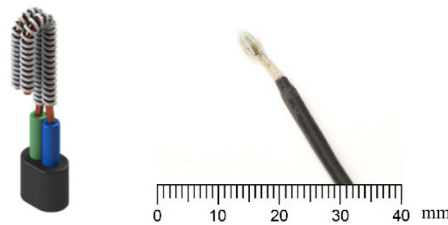


Fig. 2. CAD model (left) and picture (right) of the sensor used, Aguiar et al. [12].

An 8 bit analog-to-digital converter (ADC) uses a voltage divider to measure the voltage drop between the electrodes, returning a value between 0 and 1023, that can be converted to voltage drop, but will be left as is for easier result analysis and comparison.

To corroborate the sensor measurements, a Logitech C920 webcam was placed facing the intake front of the heat exchanger, as shown in Fig. 3. This camera is perpendicular to and leveled with the center of the HX for lower image distortion. Fixed Illumination directed towards the HX eliminates any significant noise that exterior lighting fluctuations could introduce into the system.

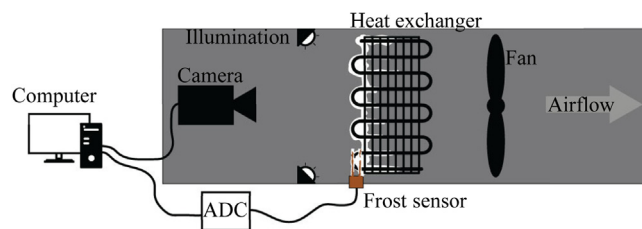


Fig. 3. Experimental setup scheme.

The images are captured and processed in MATLAB version R2018b according to the diagram shown in Fig. 4. First MATLAB creates the webcam object and specifies the fixed capture properties (to avoid automatic adjustments). A snapshot is then taken and properly cropped to the HX area. The image converted in a B&W binary image, using a threshold. The threshold should be adjusted along with the capture properties and lighting so that the frosted HX is almost completely white and the dry HX is almost completely black in the B&W binary image. The difference between grayscale and binary image is that a grayscale has a value between 0 and 255 for every pixel, and binary has only a value of 1 or 0 for every pixel. Finally, the black pixels are counted, and the proportion of black to white pixels is calculated to fit between 0 (for a fully black image) and 1023 (for a fully white image), so that the camera frost measurement values are in the same range of those measured by the sensor’s ADC.

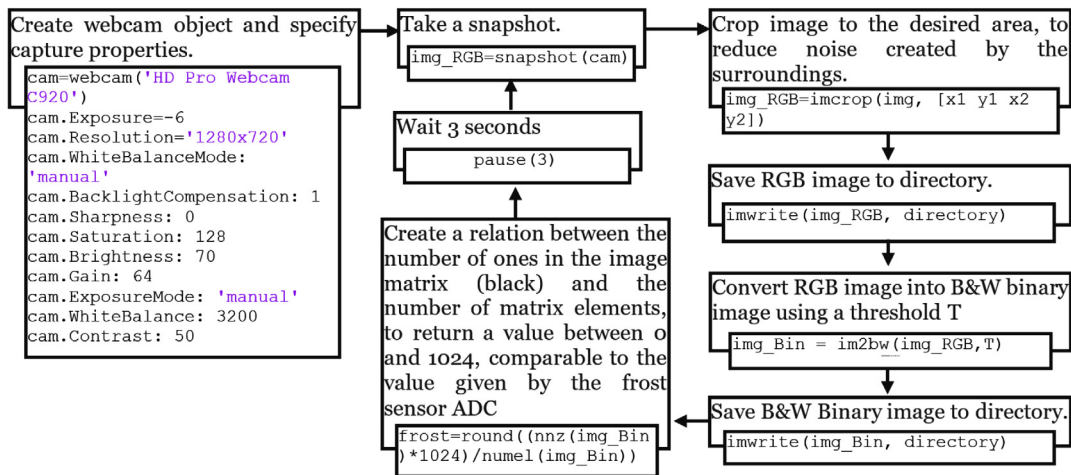


Fig. 4. Block diagram detailing the image processing procedure.

Because the experimental setup has been designed for fast frost and defrosting cycles, an image sample is captured, processed, and stored in RGB and B&W binary every three seconds.

The results of one capture are shown in Fig. 5. Some noise is created by the temperature and humidity sensor, as well as by some fin damage in the HX, although these values are constant, and will not affect the readings in a significantly.

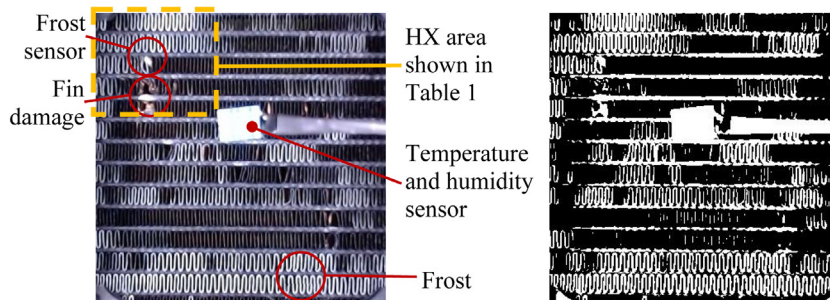


Fig. 5. RGB image (a) and processed B&W Binary image (b).

In the results section, only the area highlighted in Fig. 5 will be shown in Table 2, although the curves and values discussed have been calculated with the whole HX surface. Nonetheless, this method allows for multi-zone frost formation analysis, which can be useful for testing multiple sensors simultaneously and comparing their values with the respective zones in which they are placed.

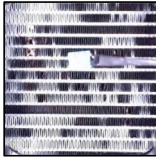
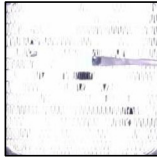
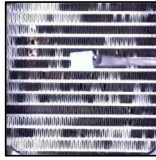
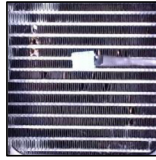
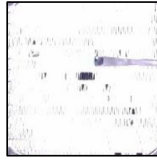

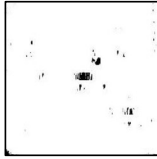

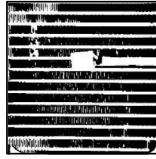
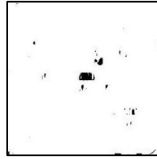
3. Results and discussion

Several frost–defrost cycles were performed with variation in fan speeds and air relative humidity for different cycles to obtain more representative test data. In Fig. 6, data crossing between the resistive sensor values and image processing values is presented for five consecutive frost–defrost cycles.

The relation between the sensor and image processing values is clear, even with irregular frost formation. Although the camera only has a slight variation between dry and wet HX, the sensor properly distinguishes these two phases. The different levels of frost detection of the camera are related to the conditions in which the frost was formed (air velocity and relative humidity) and the frost accumulated before each defrosting shown in Table 1.

When comparing the values of Fig. 6 and Table 1, the different values for frost detection via image processing become evident. 2nd and 5th cycles start a defrost with the HX almost completely blocked by frost, while a defrosting operation was initiated in 1st, 3rd and 4th cycles with far less frost accumulation. To analyze the phases of each cycle, the 2nd frost–defrost cycle is detailed in Fig. 7.

Table 1. Frost accumulation before a defrosting operation was initiated for each of the five frost–defrost cycles.

First cycle	Second cycle	Third cycle	Fourth cycle	Fifth cycle
				
				

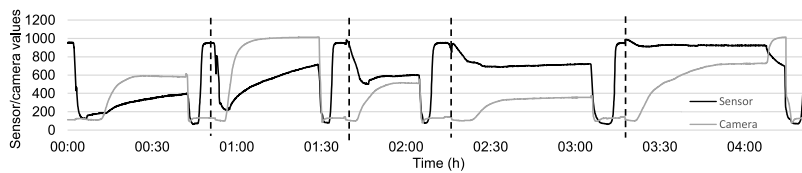


Fig. 6. Sensor and image processing values for five consecutive frost–defrost cycles.

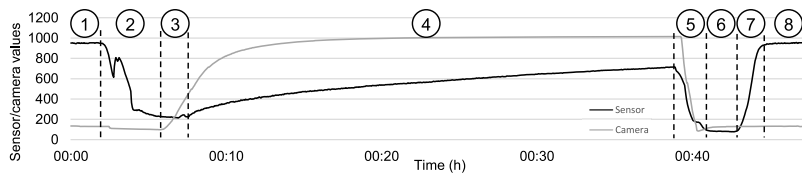


Fig. 7. Sensor and image processing values for a single frost–defrost cycle.

This cycle can be divided in 8 phases, (in which phase 8 is the phase 1 of the next cycle). First the HX starts dry (1), then, as its surface temperature lowers below the dew point, condensation starts to happen on the HX surface and is detected by the sensor (2). Lower temperatures result in frost formation being detected by the camera (3). Because the frost formation distribution is uneven across the HX, there is a delay in the frost detection by the sensor (4). A defrosting operation is initiated, resulting in the accumulated frost melting (5), and accumulation of water that saturates the sensor (6) until water evaporate (7) and the HX becomes dry again (8). The HX zone where the sensor was placed (cropped according to the area mentioned in Fig. 5) is shown across the different phases in Table 2.


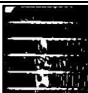

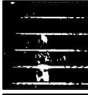






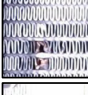








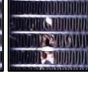


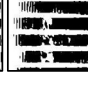
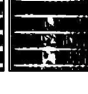

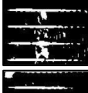

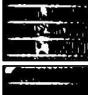


Because visible processes happen in phases 3, 4 and 5, more than one image is used to illustrate the phase. In the other phases, no visible noticeable change happens.

In the third phase, it is clear why the sensor did not detect frost immediately at the same time the frost formation started happening, as only in the fourth phase, frost started accumulating in the zone the sensor was placed.

The very slight variation in the image processing values during condensation are related to the HX surface light reflecting properties varying for a dry, wet, and frozen (with clear ice) surface.

It is also possible to analyze through Fig. 5, and the images in Tables 1 and 2 that the frost formation is not only uneven across the HX, but also has a pattern that repeats itself across cycles and phases. This frost formation map will most likely be different for every system and should be taken in consideration for the application of frost detection sensors.

Table 2. Samples of the image processing across phases.

Phase	RGB Images	B&W Binary Images
1		
2		
3	  	  
4	  	  
5	   	   
6		
7		
8		

4. Conclusions

In this paper, an image recognition method for frost detection corroborated by data obtained from other frost sensing methods was implemented. The main conclusions are:

- (1) Image recognition is a reliable and effective way of frost detection, although it is not as compact, low-cost, and resistant to damage as a small sensor. Its use for application in a research environment is ideal and allows for data to be crossed with that of other sensors. In the present work, it allowed for a better understanding of frost formation in a particular HX, and interpretation of the results obtained from the resistive sensor.
- (2) Image recognition allows for a creation of a frost formation map that can be used to better apply sensors in a HX. It should be taken into consideration that frost formation in zones with rapid frost formation might result in a frost detection that happens before the ideal time to perform a defrosting operation, and frost sensing in zones with slow frost formation might result in frost detection that happens after the ideal time to perform a defrosting operation.
- (3) Control methods might use previously obtained frost maps to calibrate defrosting operations to the sensor measurements to control defrosting in the most efficient way possible.
- (4) The resistive sensor is an effective way of detecting frost formation in heat exchangers, and the image sensing data corroborates this claim.
- (5) This method was tested in a copper HX covered in black paint, effectiveness in non-treated metallic HXs should be lower, because of the lower contrast between HX surface and frost layer, but this has not been tested yet.

CRedit authorship contribution statement

Martim Aguiar: Investigation, Formal analysis, Validation, Writing – original draft. **Pedro Dinis Gaspar:** Writing – review & editing. **Pedro Dinho da Silva:** Supervision, Data curation.

Declaration of competing interest

The authors declare that they have no known competing financial interests or personal relationships that could have appeared to influence the work reported in this paper.

Acknowledgments

This work has been supported by the project Centro-01-0145-FEDER000017 -EMaDeS -Energy, Materials and Sustainable Development, co-funded by the Portugal 2020 Program (PT 2020), within the Regional Operational Program of the Center (CENTRO 2020) and the EU through the European Regional Development Fund (ERDF). The authors thank the opportunity and financial support to carry on this project to Fundação para a Ciência e Tecnologia (FCT) and R&D Unit “Centre for Mechanical and Aerospace Science and Technologies” (C-MAST), under project UIDB/00151/2020.

This study is within the activities of project “PrunusPós - Optimization of processes for the storage, cold conservation, active and/or intelligent packaging and food quality traceability in post-harvested fruit products”, project n.º PDR2020-101-031695, Partnership n.º 87, initiative n.º 175, promoted by PDR 2020 and co-funded by EAFRD within Portugal 2020.

References

- [1] C. Melo, e D.L. Hermes, C.J. Silva, Experimental study of frost accumulation on fan-supplied tube-fin evaporators, *Appl Therm Eng* 31 (2011) 1013–1020.
- [2] C.J.L. Hermes, R.O. Piuccio, e C. Barbosa Jr., J.R. Melo, A study of frost growth and densification on flat surfaces, *Exp Therm Fluid Sci* 33 (2009) 371–379.
- [3] W. Wang, J. Xiao, Q.C. Guo, e Y.C. Lu, W.P. Feng, Field test investigation of the characteristics for the air source heat pump under two typical mal-defrost phenomena, *Appl Energy* 88 (2011) 4470–4480.
- [4] M.L. Aguiar, P.D. Gaspar, P.D. Silva, Frost measurement methods for demand defrost control systems: A review, IAENG, London, 2018.
- [5] Y. Ge, Y. Sun, W. Wang, J. Zhu, e J. Li, L. Liu, Field test study of a novel defrosting control method for air-source heat pumps by applying tube encircled photoelectric sensors, *Int J Refrig* 66 (2016) 133–144.
- [6] J.H. Jarrett, A new demand defrost control for domestic forced draft refrigerator freezers and freezers, *IEEE Trans Ind Appl* 1 (3) (1972) 356–364.
- [7] L. Zhu, Z. Cao, W. Zhuo, R. Yan, A new dew and frost detection sensor based on computer vision, 2013.
- [8] Zhaoyang Li, Wei Wang, Yuying Sun, Shiquan Wang, Shiming Deng, Yao Lin, Applying image recognition to frost built-up detection in air source heat pumps, *Energy* 233 (2021) 121004, <http://dx.doi.org/10.1016/j.energy.2021.121004>.
- [9] M.L. Aguiar, P.D. Gaspar, P.D. Silva, A.P. Silva, A.M. Martinez, Medium materials for improving frost detection on a resistive sensor, *Energy Rep* 6 (Suppl. 8) (2020) 263–269, <http://dx.doi.org/10.1016/j.egy.2020.11.258>.
- [10] P.D. Gaspar, P.D. Silva, e L.P. Nunes, J. Andrade, Monitoring device of ice formation in evaporator surface of refrigeration systems, in: VI Ibero-American refrigeration sciences and technologies, Coimbra - Portugal, 2016.
- [11] D. Caetano, e P.D. Gaspar, P.D. da Silva, Experimental testing of a resistive sensor for monitoring frost formation in refrigeration systems, in: Em X Iberian congress & VII congress on Ibero-American refrigeration sciences and technologies, Valencia, 2018.
- [12] Martim Aguiar, Pedro Gaspar, Pedro Silva, Testing of a resistive sensor with fabric medium for monitoring frost formation in refrigeration systems, *Procedia Environ Sci Eng Manag* 8 (1) (2021) 205–214.